Simulation of Wave Impact on Three-Dimensional Horizontal Plate Based on SPH Method

Zheng Kun(郑坤)[1,2], *Sun Jiawen*(孙家文)[1,2], *Chen Changping*(陈昌平)[3*], *Sun Zhaochen*(孙昭晨)[2], *Ren Xifeng*(任喜峰)[2]

1. National Marine Enviromental Monitoring Center, Dalian, 116023, P. R. China;
2. State Key Laboratory of Coastal and Offshore Engineering, Dalian University of Technology, Dalian, 116024, P. R. China;
3. School of Ocean and Civil Engineering, Dalian Ocean University, Dalian, 116023, P. R. China

(Received 9 April 2014; revised 25 June 2014; accepted 3 July 2014)

Abstract: An improved three-dimensional incompressible smooth particle hydrodynamics (ISPH) model is developed to simulate the impact of regular wave on a horizontal plate. The improvement is the employment of a corrective function to enhance angular momentum conservation in a particle-based calculation. And a new estimation method is proposed to predict the pressure on the horizontal plate. Then, the model simulates the variation characteristics of impact pressures generated by regular wave slamming. The main features of velocity field and pressure field near the plate are presented. The present numerical model can be used to study wave impact load on the horizontal plate.

Key words: incompressible smoothed particle hydrodynamics (ISPH); wave impact; three-dimensional horizontal plate

CLC number: TV139.2 **Document code**: A **Article ID**: 1005-1120(2014)06-0701-09

1 Introduction

The coastal and offshore engineering structure security problem have recently become a research hot issue, especially the wave impact problems. The extreme wave impact forces caused by strong wave slamming may lead to tremendous damage of the open structures. The mechanics of wave slamming is very complicated because of its strong nonlinearity, instantaneous effect, fluid viscosity, turbulence and miscibility of fluid and gas, etc. Many researchers have estimated the wave impact load[1-7].

With the rapid development of the computer technology and computational fluid dynamics (CFD) methods, seeking numerical solutions to the N-S equations that include the imcompression and viscosity of the fluid has become a popular way to estimate the wave impact force on structures. Most of the existing numerical models solving the N-S equations are based on grid methods. Ren and Wang[8,9] introduced a numerical model for wave and two-dimensional horizontal plate based on volume of fluid (VOF) method, and improved the boundary treatments for both impact and wave, which turns out a more satisfactory result. Christakis and Kleefsman, et al.[10,11] calculated the impact load between the fluid and the structure utilizing an improved VOF method. Hu and Kashiwagi reported some good results for impacting force calculation using the compact pattern of the constrained interpolation profile-conservatives semi-Lagrangian scheme with third-order polynomial function(CIP-CSL3) method. However, the above methods are all

Foundation items: Supported by the National Science Foundation of China (51109022); the National Science Foundation of Liaoning Province (201202020); the Key Laboratory Foundation of Dalian University of Technoloty (LP12005).

* **Corresponding author**: Chen Changping, Associate Professor, E-mail: ccp@dlou.edu.cn.

based on grid, which is difficult to solve large deformation free surface flows, such as wave breaking and impacting.

Smoothed particle hydrodynamics (SPH) is a meshfree, Lagrangian, particle method, which is particularly suited to the solution and modelling of large scale, complex free surface fluid flows. From compressible flows to incompressible flows, the SPH method shows reliable performance. Monaghan, et al.[12] used the weakly compressible SPH (WCSPH) method to simulate the solitary wave propagating along the beach. Liu, et al.[13] used it to simulate liquid sloshing. Dalrymple and Rogers[14] applied a large eddy simulation(LES) model to wave propagation and interaction with coastal defence. Although WCSPH predicted some highly transient flows quite well, notably dam break flows, pressures were extremely noisy and the method highly dissipative. An important development was made by Vila[15] who introduced a Riemann formulation between interacting particles and reducing pressure noise markedly. Gao and Ren, et al.[16] employed corrected smoothed particle hydrodynamics mothed (CSPM) and Riemann solution to investigate regular wave slamming on an 2D open-piled structure. The ISPH method with properties of noise-free pressure field and bigger time step limits is also preferable in free-surface flow simulations. Shao and Gotoh[17] simulated the coupled motion between progressive wave and floating curtain-wall type break water with consideration of turbulence effect through a LES model. Lee, et al.[18] applied a so-called truly incompressible SPH (TISPH) method to simulate a 2D dam break. Sun, et al.[19] improved ISPH mothod to investigate regular wave impact on a 2D horizontal plate.

Although SPH has been applied to simulation of variety engineering problems, it is well-known by the SPH developers that numerical instabilities and solid boundary issue are the most need to solove in SPH[20].

In wave-structure interacting problems, the domain of interest has, in general, solid boundaries and free surfaces. The SPH formulations being valid for all interior particles are not necessarily accurate for particles close to the domanin boundary and free surface since the kernel function is truncated by the boundary. Therefore, boundaries need to be treated properly to avoid penetration of fluid particles into boundary walls and to convert the shortcoming of kernel truncation at boundaries. Hence, serveral different approaches have been used for the boundary treatment such as specular reflections, or bounceback of fluid particles with the boundary walls[21], Lennard-Jones potential (LJP) type force as a repulsive force[12,22], ghost particles[23-25], and multiple boundary tangent (MBT) method[26].

A 3D numerical wave flume based on improved ISPH method is described in the paper. The improved ISPH model is applied to the simulation of regular wave impacting on a three-dimensional horizontal plate. The numerical wave impact force results are vertification with the experimental results. The main features of velocity field and pressure field near the plate are presented.

2 Incompressible SPH Model

2.1 Governing equations

In the ISPH method, the Navier-Stokes equations are solved in Lagrangian form as follows

$$\nabla \cdot \boldsymbol{U} = 0 \tag{1}$$

$$\frac{\mathrm{d}\boldsymbol{U}}{\mathrm{d}t} = -\frac{1}{\rho}\nabla P + \boldsymbol{F} + \nu_0 \nabla^2 \boldsymbol{U} \tag{2}$$

where P is the pressure, ρ the density, $\boldsymbol{U}$ the particle velocity, ν_0 the laminar kinematic viscosity, and $\boldsymbol{F}$ the extra body force.

The SPH method is based on the interpolation theory. In SPH, the fundamental principle is to estimate any function $A(r)$, and its gradient in the form

$$A(r) = \sum_j m_j \frac{A_j}{\rho_j} W(r - r_j, h) \tag{3}$$

$$\nabla A(r)=\sum_j m_j\frac{A_j}{\rho_j}\nabla_i W(r-r_j,h) \tag{4}$$

where $W(r-r_j,h)$ is the kernel function, $\nabla_i W(r-r_j,h)$ the gradient of the kernel with respect to the position of particle i. In the paper, we use cubic spline kernel function, it can be defined as follows

$$W(R,h)=\alpha_d\times\begin{cases}\frac{2}{3}-R^2+\frac{1}{2}R^3 & 0\leqslant R<1\\ \frac{1}{6}(2-R)^3 & 1\leqslant R<2\\ 0 & R\geqslant 2\end{cases} \tag{5}$$

where $R=r/h$, for 3D problems, the normalization factor takes the value, $\alpha_d=3/2\pi h^3$, h is the smooth length.

2.2 Solution procedure

In the solution process of pressure P, we will divide each time-step into two implementation steps. The method is similar to the moving particle semi-implicit method.

The first step, the intermediate velocity $\boldsymbol{u}^*$ generated by the non-pressure items is solved using the source item at the time of $t=n$.

$$\frac{\boldsymbol{u}^*-\boldsymbol{u}^n}{\mathrm{d}t}=\boldsymbol{g}+\upsilon_0\nabla^2\boldsymbol{u} \tag{6}$$

Then, making amendments according to continuity equation and momentum equation, we can obtain the followings

$$\boldsymbol{u}^*=\boldsymbol{u}^n+\Delta\boldsymbol{u}^* \tag{7}$$

$$\Delta\boldsymbol{u}^*=\boldsymbol{f}\Delta t \tag{8}$$

$$\boldsymbol{r}^*=\boldsymbol{r}^n+\boldsymbol{u}^*\Delta t \tag{9}$$

For the second step, assume that $\boldsymbol{u}^{n+1}=\boldsymbol{u}^*+\Delta\boldsymbol{u}$, where $\Delta\boldsymbol{u}$ is the change of speed generated by the pressure item

$$\Delta\boldsymbol{u}=-\frac{1}{\rho^*}\nabla P^{n+1}\Delta t \tag{10}$$

To introduce this speed item into the continuity equation, Poisson equation for pressure can be derived as follows

$$\nabla\left(\frac{1}{\rho^*}\nabla P^{n+1}\right)=\frac{\rho-\rho^*}{\rho\Delta t^2} \tag{11}$$

where ρ and ρ^* are the initial and temporal fluid density of each partiles, respectively, calculated as

$$\rho_i=\sum_j m_j w_{ij} \tag{12}$$

By using the Poisson equation for pressure, we can obtain the speed generated by pressure item and thus derive the speed $\boldsymbol{u}^{n+1}$ and $\boldsymbol{r}^{n+1}$ at the time of $t=n+1$.

$$\boldsymbol{u}^{n+1}=\boldsymbol{u}^n-\frac{\Delta t}{\rho^*}\nabla p^{n+1} \tag{13}$$

The improved form of the pressure gradient item proposed by Shao is used

$$\nabla\cdot\left(\frac{1}{\rho^*}\nabla P^{n+1}\right)_i=\sum_j m_j\frac{8}{(\rho_i+\rho_j)^2}\frac{P_{ij}\boldsymbol{r}_{ij}\cdot\nabla W_{ij}}{|\boldsymbol{r}_{ij}|^2+\eta^2} \tag{14}$$

To complete the time-step, a second-order time marching scheme is used

$$\boldsymbol{r}^{n+1}=\boldsymbol{r}^n+\Delta t\left(\frac{\boldsymbol{u}^{n+1}+\boldsymbol{u}^n}{2}\right) \tag{15}$$

where $P_{ij}=P_i-P_j$, $\boldsymbol{r}_{ij}=\boldsymbol{r}_i-\boldsymbol{r}_j$, $\boldsymbol{r}_{ij}$ is a small quantity that guarantees the denominator not being zero in the middle steps of calculation, generally takes 0.1 time of the smooth length. The coefficient matrix of the equation is symmetric positive definite and the main diagonal is dominant. Therefore, it is convenient to use high-efficiency calculation method for solution. In the paper, biconjugate gradient method is employed[27,28].

2.3 Corrected ISPH model

All computational models for simulating fluid flows are based on the fundamental principles of physics including mass and momentum conservation. Particle methods are not an exception; however, because of particle-based discretization, local conservation of momentum may not be guaranteed in a particle-based calculation. In the ISPH method, the pressure interacting forces are anti-symmetric in addition to being radial; thus, both linear and angular momentum are preserved in case of pressure interacting forces[18]. On the other hand, the viscous interacting forces that are obtained from a tensor-type strain-based viscosity do not necessarily act along the position vector $\boldsymbol{r}_{ij}$; therefore, conservation of angular momentum will not be ensured in an ISPH calculation with

tensor-type strain-based viscosity term.

Khayyer, et al.[29] employed a corrective technique to correct the gradient of kernel function in calculating viscous forces to guarantee the conservation of angular momentum. In the paper, we use a correct method the same as Khayyer's. The corrected gradient of kernel function should be used to calculate the force in the equation of motion instead of the gradient of the kernel $\nabla_i W(r-r_j,h)$. The corrected gradient of kernel functions are as follows

$$\nabla_i \widetilde{W}_{ij} = L_i \nabla_i W_{ij} \tag{16}$$

$$L_i = (\sum V_j \nabla_i W_{ij} \otimes (\boldsymbol{r}_j - \boldsymbol{r}_i))^{-1} \tag{17}$$

Therefore, the final form of Eqs. (2,14) can be written as

$$\frac{\mathrm{d}U_i}{\mathrm{d}t} = -\sum_j m_j \left(\frac{p_i}{\rho_i^2} + \frac{p_j}{\rho_j^2}\right) \widetilde{\nabla}_i W_{ij} + g_i + \sum_j m_j \frac{4\nu_0 \boldsymbol{r}_{ij} \widetilde{\nabla}_i W_{ij}}{(\rho_i + \rho_j)|\boldsymbol{r}_{ij}|^2} U_{ij} \tag{18}$$

$$\nabla \cdot \left(\frac{1}{\rho^*} \nabla P^{n+1}\right)_i = \sum_j m_j \frac{8}{(\rho_i + \rho_j)^2} \frac{P_{ij} \boldsymbol{r}_{ij} \cdot \widetilde{\nabla} W_{ij}}{|\boldsymbol{r}_{ij}|^2 + \eta^2} \tag{19}$$

2.4 Treatment of boundary conditions and free surfaces

The treatment of boundary conditions and free surface is similar to Shao's. The solid boundaries are represented by the fixed wall particles, which are similar to the fluid particles. The pressure Poisson equation is also solved on these wall particles, but their velocities are set to zero at end of each time-step. Therefore, their velocities and positions are fixed. The free surface can be easily and accurately tracked since the calculated densities at particles on the free surface drop abruptly due to lack of particles in the outer region of the free surface. The following criterion is considered for the detection of free surface particles

$$\rho = 0.99\rho_0 \tag{20}$$

In order to get exact solution to the pressure on some points on the deck, a new estimation method is applied. Based on the solid boundary described above, the particles on the deck are solved like fluid particles, but in the simulations, the sum over all the neighboring particles is replaced by the sum over the only neighboring fluid particles, only the fluid particles are considered in the pressure simulation. As shown in Fig. 1, the pressure can be written as

$$p_i = \frac{\boldsymbol{F}_j \cdot \boldsymbol{n}}{d_{\mathrm{sensor}}} \tag{21}$$

where $d_{\mathrm{sensor}} = 2h \cdot 2h$, $\boldsymbol{F} \cdot \boldsymbol{n}$ is the total force on the wall, it can be written as

$$F_j = \sum_{\mathrm{sensor}} p_j \nabla W_{ij} m_j \tag{22}$$

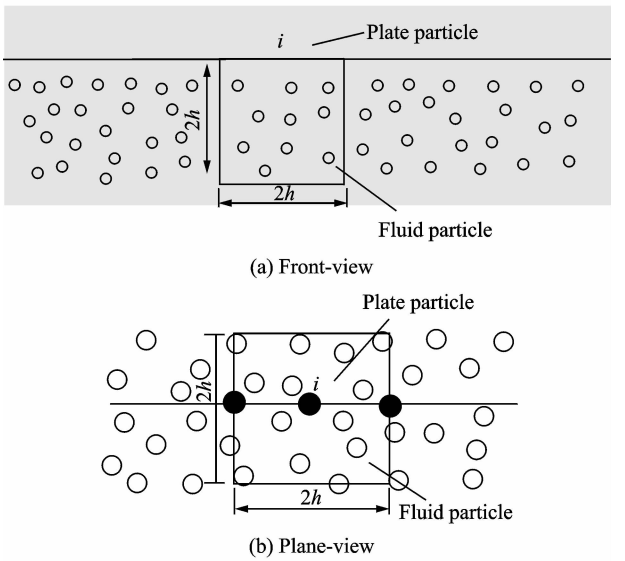

Fig. 1 Sampling area

3 Numerical Simulation

3.1 Wave-making boundary

Regular waves can be generated using a wave maker based on the linear theory. The profile of a regular wave as a function of time t is defined as Eq. (23)

$$U(t) = \frac{X_0 \omega}{2} \cos \omega t \tag{23}$$

where X_0 and ω are the amplitude and frequency of wave maker. $X_0 = H/W$, W is the transfer function. It can be written as Eq. (24)

$$W = \frac{4 \sinh^2 kd}{2kd + \sinh 2kd} \tag{24}$$

where k is wave number.

If a wave with surface elevation η_0 is produced by the wave maker, the velocity of the

wave maker should be determined as follows

$$U_0(t)=\frac{\eta_0\omega}{W} \tag{25}$$

In SPH method, the displacement of the wave maker boundary particles is to be renewed at each calculating step. Therefore, when a wave with $\eta_0=0.5\times H\times\cos\omega t$ is to be generated, the velocity and the displacement of the wave maker boundary particles should be as the Eqs. (26, 27), respectively

$$U_0(t)=\frac{1}{2}H\frac{\omega\sin\omega t}{W} \tag{26}$$

$$S_0(t)=-\frac{1}{2}H\frac{\cos\omega t}{W} \tag{27}$$

3.2 Numerical computational setup

The detailed setup of numerical flume is shown in Fig. 2. The original $x=0$ and $y=0$ point is located at the still water surface on the left side of the flume, the left hand side of the flume is the wave generation boundary, and the right hand side is an absorbing boundary featured by a slope=1∶20. All walls are no-slip boundaries. The water depth is 0.8 m, the plate model is set $0.3H$ above the still water, the distance between the leading edge of the plate and wave maker is 3.0 m, and the calculation length in horizontal direction is 5 m. The incident wave is regular wave with a height $H=0.125$ m and period $T=1.4$ s. Set the initial fluid particle spacing $dx=dy=dz=5$ cm, the total number of the particles is 231 424; water density $\rho=1\,000$ kg/m^3; gravitational acceleration $g=9.80$ m/s^2; kinematic viscosity $\nu=1.0\times10^{-6}$ m^2/s. The computing time is 40 s. A typical simulation costs about 120 h on an intel i72600 3.4 GHz CPU, 8 GB RAM PC.

And the structures are represented by blocking out appropriate mesh cells with the same size as the experiment model with the side length B of 75 cm. There are 25 pressure sensors laid out underneath the horizontal plate model, which can be seen from Fig. 3. The distance between sensors is set to be 15.0 cm, and the distance between the outer sensor and the edge of the plate is 7.5 cm.

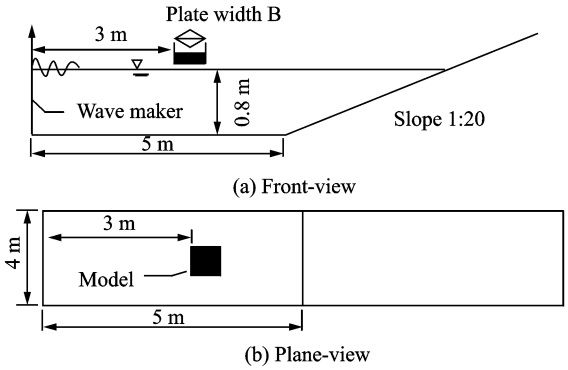

Fig. 2 Sketch of numerical calculated domain

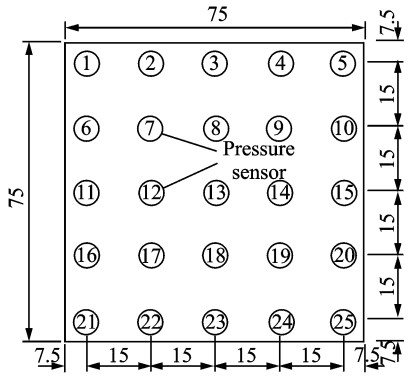

Fig. 3 Layout of pressure sensors underneath horizontal plate

4 Numerical Results

4.1 Time series of wave impact pressure comparison

Improved ISPH, standard ISPH and experimental results[30] are compared. The computed (improved ISPH and standard ISPH) and experimental results of the impact pressure time series at three transducers (1#, 9#, 13#) on the underneath of three-dimensional horizontal plate, when the incident wave height $H=12.5$ cm, wave period $T=1.4$ s and the relative clearance $\Delta h/H=0.3$, is shown in Fig. 4. In order to compare the calculation results for clarity, only 6 s impact pressure time series are shown in Fig. 3.

In Fig. 4, the large peak pressure occurs at initial contact and varies randomly from cycle to cycle even under regular wave action. At the instance of contact moment of the wave crest to the plate, the impact force is large in magnitude and short in duration. This is followed by a longer duration positive force and then by a long-duration negative force.

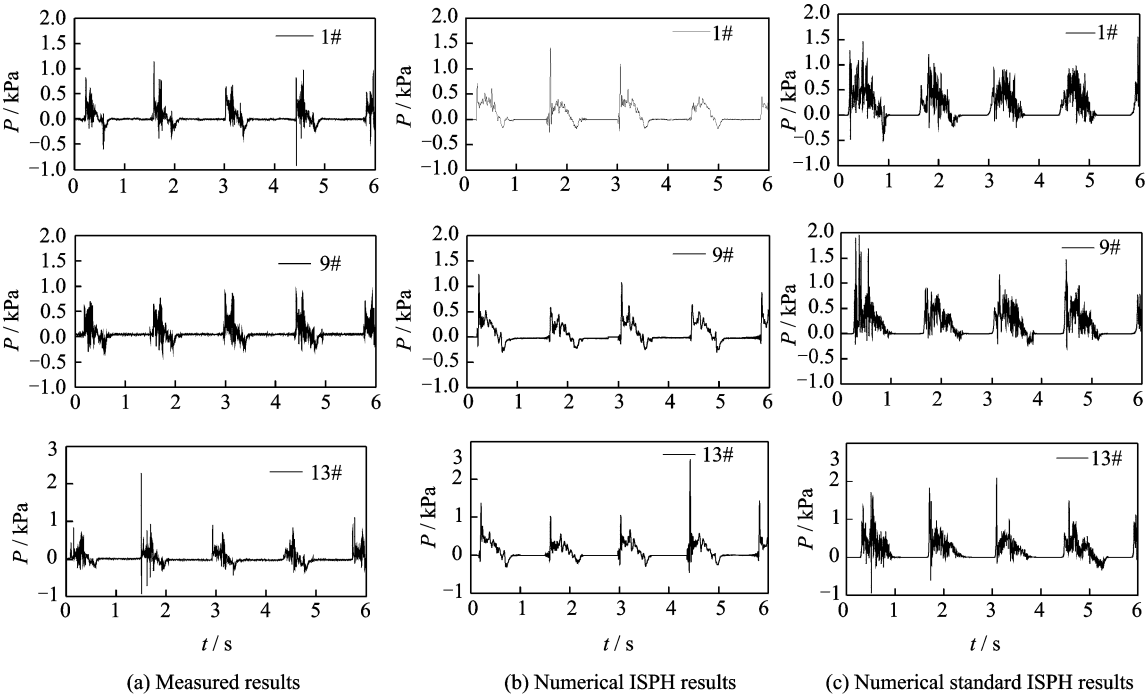

Fig. 4 Time series of wave impact pressure comparison

The impact pressures resulting from the improved ISPH simulation agree very closely with the experimental results. It can predict the magnitude of the peak pressure. The numerical result by standard ISPH exhibits large pressure oscillations, many unphysical less-than-zero pressure points after the peak pressure, which are inconsistent with the experimental results. According to the comparison, the magnitude of the peak pressure by improved ISPH has a better agreement with the experiment, and the pressure time series has fewer pressure oscillations. This ensures that the improved ISPH model is well suited for simulating the variation character of the impact pressure of the three-dimension structure under regular wave.

4.2 Velocity field and pressure distribution

Fig. 5 shows the distribution of pressure field at typical time. Fig. 6 shows the instantaneous velocity and pressure field of front view for the case of $T=1.4$ s, $H=0.125$ m. In Figs. 5—6, the pressure field is stable and the fluid particles display regularly and smoothly.

It can be seen from Figs. (a—c), at the instant $t=0.2\ T$(Fig. 6(a)), parts of the fluid par-

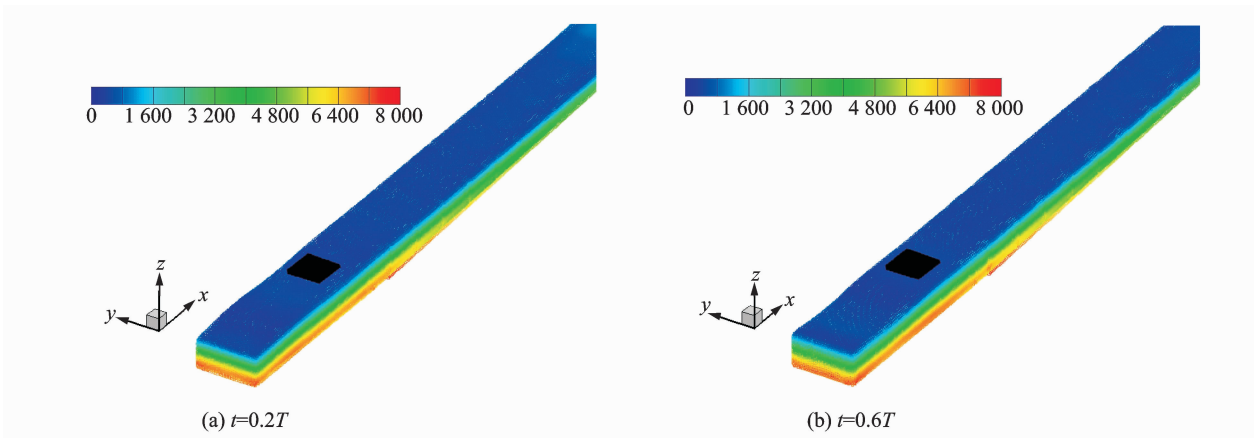

Fig. 5 Distribution of pressure field at typical time in 3D

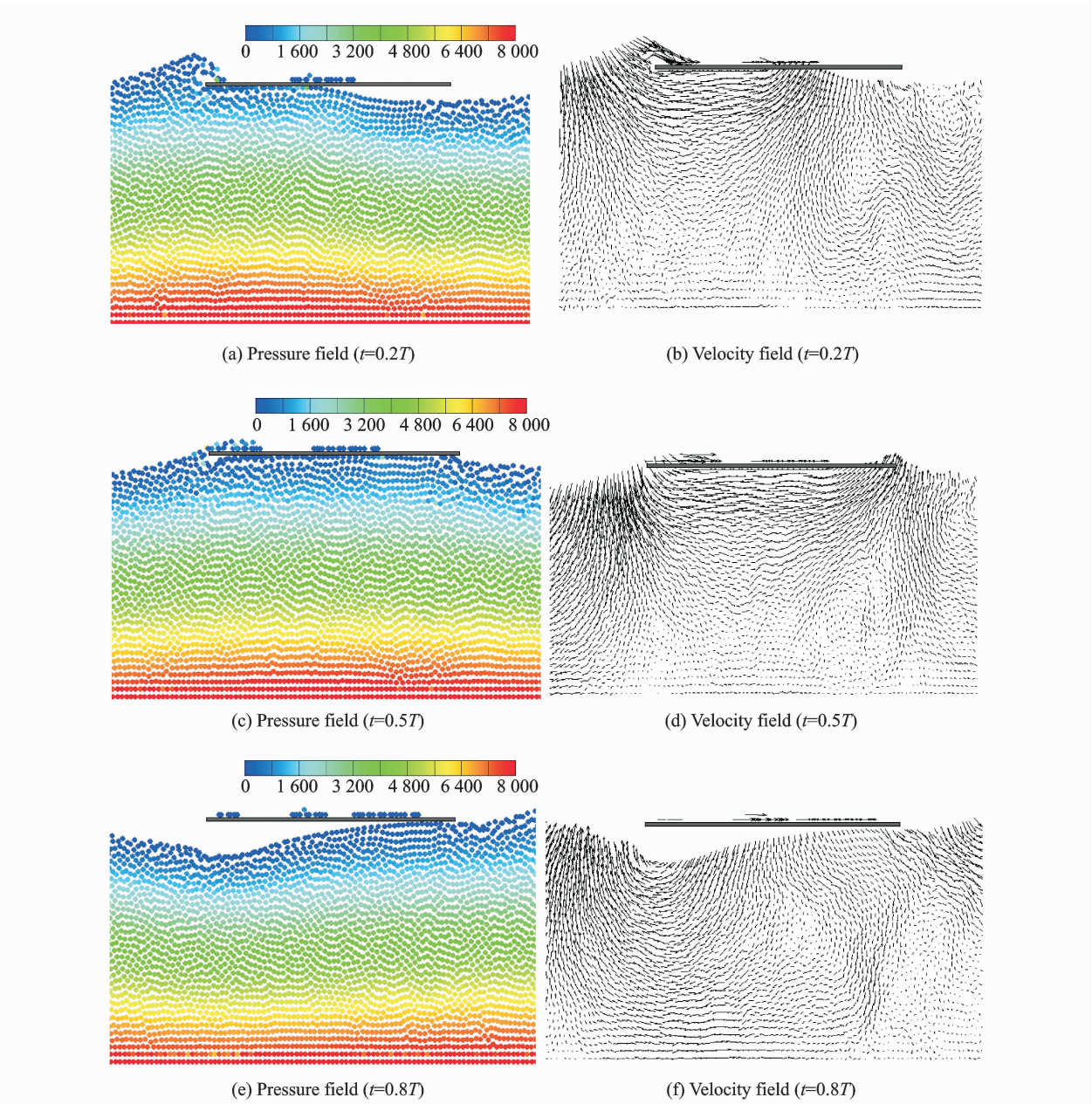

Fig. 6 Distribution of pressure and velocity field at typical time in front view

ticles influence the undersides of the horizontal plate and change their moving direction while the fluid particles not reached on the plate, particles are still moving obliquely toward the plate. At the instant $t=0.5T$ (Fig. 6 (b)), most of the fluid particles having reached on the undersides of the horizontal plate are moving forward along the underside of the plate. At the instant $t=0.8T$ (Fig. 6 (c)) shows that the fluid particles keep moving forward along the underside of the plate and separate from the underside of the plate gradually.

4.3 Distribution of impact pressure on underside of plate

When waves slam on the horizontal plate, the waves have a great deformation due to the plate influence. The pressure at different locations on the underside of the plate will move forward with the wave propagation. The maximum impact pressure and its position will change.

With the same conditions as mentioned in section 4.1, the distribution characteristics of wave impact pressure are presented in Fig. 7. The ordinate represents the distance of the plate along

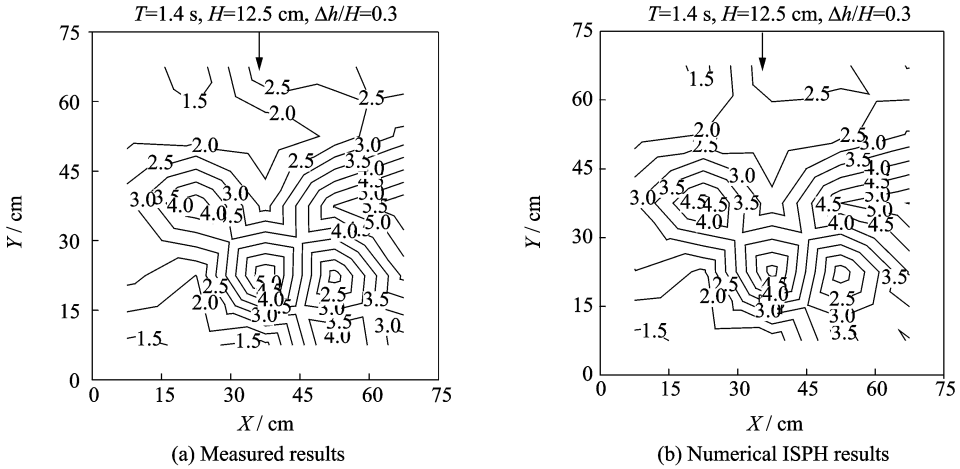

Fig. 7 Measured value and numerical value of regular wave impact pressure on underside of plate

the direction of waves propagating. The abscissa represents the distance of the plate cross the direction of wave propagating. The curve is the isoline of the significant peak pressures on the underside of the structure. The arrow indicates the direction of the wave propagating. In Fig. 7, the peak impact pressure from the numerical simulation is almost identical to the experimental results. The isoline of the significant peak pressure has a symmetrical distribution to the wave ray. The maximum pressure values underside of plate are very similar.

Numerical and experimental results[30] of the significant peak pressure (we choose the average value of the largest peak pressure as the significant peak pressure) are compared in Fig. 8. It can be seen that the significant peak pressure of numerical results are in good agreement with experimental results at most measure points.

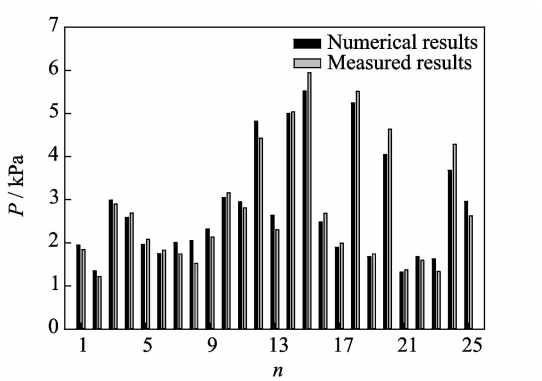

Fig. 8 Numerical and experimental results of significant peak pressure

5 Conclusions

An improved three-dimensional incompressible SPH numerical model is developed in the paper for numerical simulation of the interaction between the regular wave and the three-dimensional horizontal plate. The variation characteristics of the impact compressional of the three-dimensional structure are simulated under regular wave. It can be concluded that computation result is in good agreement with the experimental results. The new method can predict the wave impact peak pressure and the distribution of wave impact on the underside of the plate. It is shown that the improved 3D ISPH model can be used for the study of wave impact on the horizontal plate problems.

References:

[1] Wang H. Water wave pressure on horizontal plate [J]. Journal of the Hydraulics Division, 1970, 96 (10): 1997-2017.

[2] Kaplan P. Wave impact force on offshore structures: Re-examination and new interpretations [C]// Offshore Technology Conference. Houston, Texas: AAPG, 1992: 79-86.

[3] Ren B, Wang Y X. Laboratory study of random wave slamming on a piled wharf with different shore connecting structures [J]. Coastal Engineering, 2005, 52(5): 463-471.

[4] Ding Z Q, Ren B, Wang Y X, et al. Experimental study of unidirectional irregular wave slamming on the three-dimensional structure in the splash zone [J]. Ocean Engineering, 2008, 35(16): 1637-1646.

[5] Zhou Yiren, Chen Guoping, Wang Dengting. Calculation methods of uplift forces of waves on a horizontal plate[J]. The Ocean Engineering, 2004, 22(2): 26-30. (in Chinese).

[6] Chen G P, Meng Y Q, Yan S C. Experimental investigation of irregular wave uplift force on deck of exposed higher pile jetties[J]. China Ocean Engineering, 2010, 24(1): 67-78.

[7] Sun J W, Sun Z C, Liang S X, et al. Experimental study of random wave impact on a Horizontal plate [C]//20th International Offshore and Polar Engineering Conference. Beijing, China: ISOPE, 2010: 663-669.

[8] Ren Bing, Wang Yongxue. Impact of nonlinear wave on structures[J]. Journal of Dalian University of Technology, 1999, 39(4): 562-566. (in Chinese).

[9] Ren B, Wang Y X. Numerical simulation of random wave slamming on the structure in the splash zone [J]. Ocean Engineering, 2004, 31(5/6): 547-560.

[10] Christakis N, Allsop N W H, Beale R G, et al. A volume of fluid numerical model for wave impacts at coastal structures[J]. Proceedings of the Institution of Civil Engineers: Water and Maritime Engineering, 2002, 154(3): 159-168.

[11] Kleefsman T, Loots E, Veldman A, et al. The numerical simulation of green water loading including the vessel motions and the incoming wave field[C]// Proceedings of 24th International Conference on Offshore Mechanics and Arctic Engineering. Halkidki, Greece: Amer Society of Mechanical, 2005: 1-12.

[12] Monaghan J J, Kos A. Solitary waves on a cretan beach[J]. Journal of Waterway, Port, Coastal, and Ocean Engineering, 1999, 125(3): 145-154.

[13] Liu Fu, Tong Mingbo, Chen Jianping. Numerical simulation of three-dimensional liquid sloshing based on SPH method[J]. Journal of Nanjing University of Aeronautics and Astronautics, 2010, 42(1): 122-126. (in Chinese)

[14] Dalrymple R A, Rogers B D. Numerical modeling of water waves with the SPH method[J]. Coastal Engineering, 2006, 53(9): 141-147.

[15] Vila J P. Particle weighted methods and smooth particle hydrodynamics[J]. M3AS, 1999, 9(2): 161-209.

[16] Gao R, Ren B, Wang G Y, et al. Numerical modelling of regular wave slamming on subface of openpiled structures with the corrected SPH method[J]. Applied Ocean Research, 2012, 34(1): 173-186.

[17] Shao S, Gotoh H. Simulating coupled motion of progressive wave and floating curtain wall by SPH-LES model[J]. Coastal Engineering Journal, 2004, 46(2): 171-202.

[18] Lee E S, Moulinec C, Xu R, et al. Comparisons of weakly compressible and truly incompressible algorithms for the SPH mesh free particle method[J]. Journal of Computational Physics, 2008, 227(18): 8417-8436.

[19] Sun Jiawen, Liang Shuxiu, Sun Zhaochen, et al. Simulation of wave impact on a horizontal deck based on SPH method[J]. Journal of Marine Science and Application, 2010, 9(4): 372-379.

[20] Shadloo M S, Zainali A, Sadek S H, et al. Improved incompressible smoothed particle hydrodynamics method for simulating flow around bluff bodies[J]. Computer Methods in Applied Mechanics and Engineering, 2011, 200(9/10/11/12): 1008-1020.

[21] Simpson J C, Wood M. Classical kinetic theory simulations using smoothed particle hydrodynamics[J]. Phys Rev E, 1996, 54(2): 2077-2083.

[22] Monaghan J J. Smoothed particle hydrodynamics[J]. Rep Prog Phys, 2005, 68(18): 1703-1759.

[23] Morris J P, Fox P J, Zhu Y. Modeling low Reynolds number incompressible flows using SPH[J]. J Comput Phys, 1997, 136: 214-226.

[24] Colagrossi A, Landrini M. Numerical simulation of interfacial flows by smoothed particle hydrodynamics [J]. J Comput Phys, 2003, 191(1): 448-475.

[25] Takeda H, Miyama S M, Sekiya M. Numerical simulation of viscous flow by smoothed particle hydrodynamics[J]. Prog Theor Phys, 1994, 92(5): 939-960.

[26] Yildiz M, Rook R A, Suleman A. SPH with the multiple boundary tangent method[J]. Int J Numer Methods Engrg, 2009, 77(10): 1416-1438.

[27] Yuan W R, Chen P, Liu K X. High performance sparse equations with solver for unetrical linear out of core strategies and its application on meshless methods[J]. Applied Mathematics and Mechanics, 2006, 27(10): 1339-1348.

[28] Zhang Y Q, Sun Q, Li J H. An improved ICCG method for large scale sparse linear equations[J]. Chinese Journal of Computational Physics, 2007, 13(5): 581-584. (in Chinese)

[29] Khayyer A, Gotoh H, Shao S D. Corrected SPH for incompressible fluid for water surface tracking in plunging breaker[J]. Coastal Engineering, 2008: 132-143.

[30] Sun Jiawen. Experimental study and numerical simulation of wave impact on horizontal deck[D]. Dalian: Dalian University of Technology, 2011. (in Chinese)

(Executive editor: Xu Chengting)